Journal of Solid Mechanics Vol. 6, No. 4 (2014) pp. 397-409

Plastic Wave Propagation Model for Perforation of Metallic Plates by Blunt Projectiles

S. Feli*, S. Noritabar

Department of Mechanical Engineering, Razi University, Kermanshah , Islamic Republic of Iran

Received 28 July 2014; accepted 1 October 2014

ABSTRACT

In this paper, a six-stage interactive model is presented for the perforation of metallic plates using blunt deformable projectiles when plastic wave propagation in both target and projectile is considered. In this analytical model, it is assumed that the projectile and target materials are rigid – plastic linear work hardened. The penetration of the projectile into the target is divided into six stages and governing equations are derived. The analytical model shows that residual velocity, diameter of the flattening area of the projectile, and ballistic limit velocity, show close agreement with the data from experiment.

Keywords: Projectile; Target; Plastic wave; Plugging; Perforation; Impact.

1 INTRODUCTION

PENETRATION of a projectile into a target has been the interest of countless number of researchers over the years. Backman and Goldsmith [1] documents theories and experiments from the 19th century until 1978 and Ref. [2] is a more recent collection of a large number of the experimental data. Also Goldsmith [3] summarized the analytical, numerical and experimental investigations of targets subjected to nonstandard collisions, penetration and perforation of strikers.

The objective of these investigations has been the assessment of materials to provide maximum protection under attack by projectiles. This was accomplished by the firing of strikers of certain geometry and material against targets. For thin and moderately thick targets, the performance measure was the ballistic limit, i.e. the velocity at which 50% of the strikers would just barely penetrate the target.

The present research uses plastic wave theory to model the perforation of metallic plate by deformable blunt projectile striking at normal incidence with impact speeds in the sub ordnance velocity range (i.e. below 500 m/s.). In the sub ordnance velocity range, impact of projectile can cause both global deformation and localized failure of the target plate. The global deflection surrounding the impact point is defined as `dishing'. For thin to moderately thick ductile metal plates struck by a blunt projectile, the dishing occurs and the subsequent failure mechanism is either plugging (predominantly shear rupture) or discing (predominantly tensile rupture).

A projectile can be either ductile or relatively deformable in comparison with the target plate. As a ductile projectile penetrates a metal plate its front end spreads radially or mushrooms. The mushrooming of a ductile projectile striking a rigid target was analyzed by Whiffin [4] ,Taylor [5], Hashmi and Thompson [6].

Multi-stage models have been proposed to study the perforation of relatively thick plates when structural response is negligible. Awerbuch and Bodner [7] extended a three-stage model for the perforation of a plate by a

* Corresponding author. Tel.: +98 831 4274535-9; Fax: +98 831 4274542.
E-mail address: Felisaeid@gmail.com (S.Feli).

non-deformable projectile. In the first stage, only inertia and compressive forces were introduced to decelerate the effective mass of the projectile. The second stage was initiated when a shear plug of the target material was formed, during which the compressive resistance was replaced by the surrounding shear force. The projectile was subjected to the inertia and the compressive resistance of the target material as well as the shear resistance around the plug in the middle stage. This model has been further modified in Ref. [8], where a two dimensional model assumes five stages of plate penetration, namely dynamic plastic penetration, bulge formation, bulge advancement, plug formation and projectile exit. Liss et al. [9] proposed another five-stage interactive model for the penetration and perforation process, where plastic wave propagation in both the thickness and the radial directions of the plate is considered. In this model,the projectile is considered to be rigid and non -deformable whereas the target material is assumed to be rigid plastic linear work hardened. A numerical procedure is necessary to solve the equations of motion of the projectile in the five stages.

Wenexue et al [10] proposed a one- dimensional wave propagation model of plate perforation by deformable projectiles. This model assumed that the projectile and plate material are rigid-linearly strain hardened and rigid-perfectly plastic respectively. The failure mechanism in this model is plugging, dishing outside the plug is neglected. The perforation process based on deformation of projectile and plug was divided into six stages.
In the five-stage perforation model in Ref. [9], the shear wave propagation in the target plate outside the plug interface was considered. However, the structural response outside the shear plug is generally neglected in most multi-stage models [11].

In this paper, which is based on the Wenexue et al [10] model, a six-stage interactive model is presented for the penetration of blunt deformable projectiles into metallic plates where plastic wave propagation in both target and projectile is considered. The model uses the principle of linear momentum for a controlled volume. The governing equations of motion for the projectile, the plug and the region outside the plug are derived. As penetnation of the projectile causes both dishing and plugging failures in the target plate modifications have been applied to the modeling of the deformation outside the shear plug (dishing) based on the shear stress wave propagation and to the modeling of strain hardening of the projectile and target plate. Residual velocity, the flattened area of the projectile and the ballistic limit velocity predicted by the new model is compared with experimental results.

2 ANALYTICAL MODEL

2.1 Analysis of the processes

As shown in Fig. 1, the impact of a blunt projectile onto a thin or moderately thick plate target can cause both global deformation (dishing) and localized failure (Plugging) of the target plate. Consider a flat-end projectile penetrating a target. The plastic wave propagates with a speed C_p in the axial direction in the projectile and with a speed C_t in the plug. A shear stress wave also propagates in the radial direction in the outer region of the plug with a speed C_s.

The analysis assumes the projectile and target material are rigid – plastic linear work hardened. The stress- strain relation of the projectile is written as:

$$\sigma_p = \mathrm{A_p} + \mathrm{B_p} \cdot \varepsilon_{\mathrm{p}} \tag{1}$$

In normal perforation, the projectile is considered to be in a state of one-dimensional stress so the plastic wave speed is determined as following equation [12]:

$$C_p = \left(\frac{1}{\rho}\frac{\partial \sigma_x}{\partial \varepsilon_x}\right)^{\frac{1}{2}} = \left(\frac{\mathrm{B_p}}{\rho_p}\right)^{\frac{1}{2}} \tag{2}$$

Accordingly, stress- strain relationship in the target plate is:

$$\sigma = \mathrm{A_t} + \mathrm{B_t} \cdot \varepsilon_{\mathrm{p}} \tag{3}$$

A plug is formed as the plate deforms. Within the plug, the deformation is assumed to be planar and the material is compressible, a state of one-dimensional strain is assumed for the plug material. Based on the Von Mises yield criterion and considering the fact that plastic deformation occurs in a constant volume, the one-dimension relationship between axial stress and axial strain is given by [12]:

$$d\sigma_x = K_t d\varepsilon_x + \frac{2}{3} d\sigma \tag{4}$$

where K_t is the bulk modulus of target material. Therefore, the speed of the plastic wave is computed as:

$$C_t = (\frac{1}{\rho_t} . \frac{\partial \sigma_x}{\partial \varepsilon_x})^{1/2} = (\frac{K_t}{\rho_t} + \frac{2}{3\rho_t} B_t)^{\frac{1}{2}} \tag{5}$$

The shear stress wave propagation speed, C_s in the outer region of the plug is:

$$C_s = (\frac{1}{\rho} \frac{\partial \tau}{\partial \gamma})^{\frac{1}{2}} = (\frac{B_t}{3\rho_t})^{1/2} \tag{6}$$

Fig.1 illustrates plug formation. The regions of the target in front of the projectile and on either side of the plastic wave are termed the deformed and non-deformed sections. Behind the wave front, the deformed plug has a particle velocity V_1 equal to the interface velocity.

At the periphery of the deformed plug there is a fracture shear stress τ_f. Ahead of the plastic wave front, the non-deformed plug is accelerated to a velocity V_4 and the stress in the wave front is the yield stress under one-dimensional strain. The diameter of the plug is equal to that of the deformed projectile.

During the penetration, the tip of the projectile deforms and the propagation of the plastic wave produces the deformed and rigid section in the projectile. The deformed section of the projectile and the plug move together with a velocity equal to V_1 and the non-deformed section moves with the velocity of V_7. The deformation of the projectile during the penetration depends on the plastic wave speed and can be categorized in the following stages [6]:

Erosion	*if* $V_s \geq C_p$
Flattening and shearing	*if* $V_s < C_p$
Rigid motion	*if* $V_s = 0$,that $V_s = V_7 - V_1$

Deformation and motion of the plug occurs in two stages, a plug formation $V_r > 0$ and a plug ejection $V_r = 0$ i.e. $V_r = V_1 - V_4 = 0$.

As shown in Fig. 1, the outer region of the plug is deformed continuously with the velocity of V_3 and its radius increases as the shear plastic wave propagates.

2.2 *Governing equations*

By considering the linear momentum equation for a controlled volume containing the projectile and plug and neglecting the friction force during the penetration process, we can write [13]:

$$F = \frac{\partial M}{\partial t} + \phi \tag{7}$$

where:

F : Total force exerted on a fixed part of a material instantaneously in a control volume.

$\frac{\partial M}{\partial t}$: Time rate of change of total linear momentum inside the control volume.

ϕ : Net out flux of linear momentum through the control surface.

As shown in the flow chart, Fig. 2, the perforation process can be divided into six stages. This process will be continuing according to one of paths shown in Fig. 2. This depends on the plastic wave speed and relative velocity of the projectile and plug. In each stage, equations of motion will be derived.

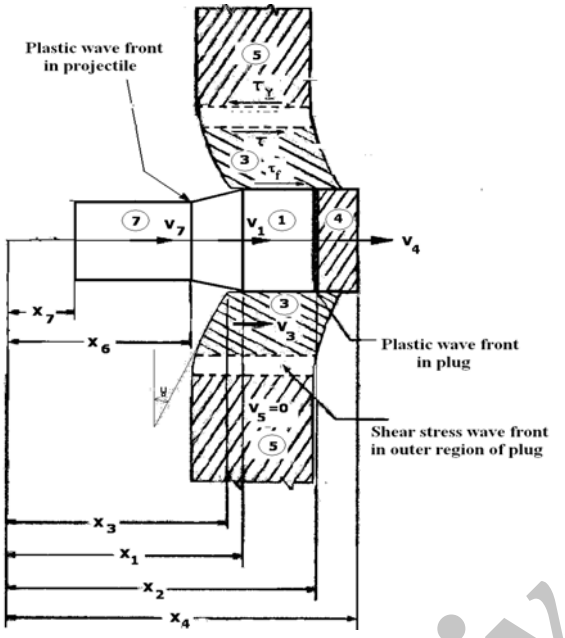

Fig. 1
Deformation of the projectile and target at perforation process.

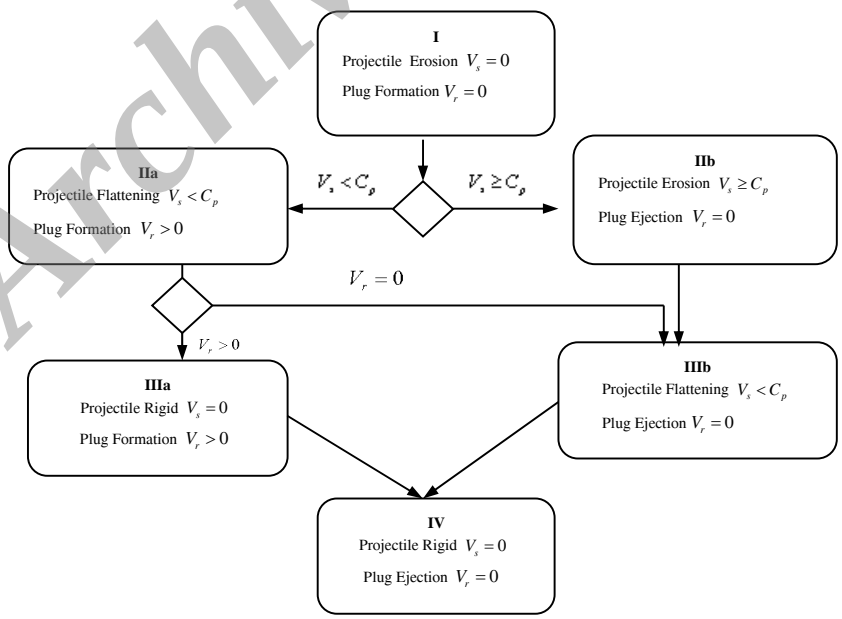

Fig. 2
Six-stage perforation process assumed in the theoretical model.

Stage I: Projectile erosion - plug formation

This stage starts when the relative velocity of the projectile is more than the plastic wave speed and the plastic wave propagates into the plug. In this stage, the projectile starts to erode and plastic deformation occurs in the section of plug where the plastic wave propagates, Fig. 3.

The principle conservation of momentum at the interface surface of the projectile and plug can be used to compute the minimum initial velocity for erosion of projectile tip as follows;

$$V_{p_0} = V_{7\ t=0} = C_p(1+\frac{\beta}{\mu})- \mu + \frac{\beta U_P}{\mu} \tag{8}$$

where $U_p = \frac{\sigma_p}{\rho_p C_p}, \beta = \frac{\rho_p C_p}{\rho_t C_t}$, and $\mu = \frac{A}{A_0}$.

The increase in the cross-sectional area of the projectile- plug interface surface is equal to:

$$\mu = \frac{A}{A_0} = \left(1-\frac{V_7}{C_p}\right)^{-1} \tag{9}$$

The linear momentum of the projectile (M_7), deformed (M_1) and non-deformed plug (M_4) are computed as follow:

$$M_7 = \rho_P \cdot A_0 \cdot (X_1 - X_7) \cdot V_7 \tag{10}$$
$$M_4 = \rho_t \cdot \mu \cdot A_0 \cdot (X_4 - X_2) \cdot V_4 \tag{11}$$
$$M_1 = \rho_t \cdot \mu \cdot A_0 \cdot (X_2 - X_1) \cdot V_1 \tag{12}$$
$$M_t = M_1 + M_4 + M_7$$

External shear force exerted on the periphery of the deformed plug is equal to:

$$F = -\pi \cdot \mu^{\frac{1}{2}} \cdot D_0 .(C_t \cdot t) \cdot \tau_f \tag{13}$$

In this equation, τ_f is failure shear stress of the target material. Net out flux of linear momentum through the control surface or erosion rate of the projectile is equal to:

$$\phi = (V_7 - V_1) \cdot V_1 \cdot \rho_p \cdot A_0 \tag{14}$$

By considering the principle of linear momentum Eq. (7) ,we have:

$$\frac{\partial M_t}{\partial t} + \phi = F \quad , \quad \frac{\partial M_7}{\partial t} = -\sigma_P . A_0 \quad , \quad \frac{\partial M_4}{\partial t} = \sigma_t . \mu . A_0 \tag{15}$$

By substituting Eqs. (10) to (14) in Eq. (15) and simplification, governing equations for calculation of V_1, V_4, V_7 are as bellow:

$$\rho_t \mu . A_0 . C_t . t \frac{dV_1}{dt} = -\pi . \mu^{1/2} . D_0 . (C_t . t) . \tau_f + \rho_P . A_0 . (V_7 - V_1)^2 - \rho_t . \mu . A_0 . C_t . (V_1 - V_4)$$
$$+(A_P + B_P) . A_0 - \{\frac{2}{3} . A_t - (K_t + B_t) . Ln \frac{(X_4 - T_0 + C_t . t - X_1)}{C_t . t}\} . A_0 . \mu \tag{16}$$

$$\rho_t.(T_0 - C_t.t).\mu.A_0 \frac{\mathrm{dV_4}}{\mathrm{dt}} = \{\frac{2}{3}.A_t - (K_t + B_t).Ln\frac{(X_4 - T_0 + C_t.t - X_1)}{C_t.t})\}.A_0.\mu) \quad (17)$$

$$\frac{\mathrm{dV_7}}{\mathrm{dt}} = -\frac{A_P + B_P}{\rho_P.L} \quad (18)$$

Rate of change in projectile length is equal to:

$$\frac{dL}{dt} = \frac{d}{dt}(X_1 - X_7) = V_1 - V_7 \quad (19)$$

In this stage, the rate of projectile flattening is equal to zero. This stage continues until:

$$V_7 - V_1 < C_P \quad or \quad V_r = V_1 - V_4 = 0$$

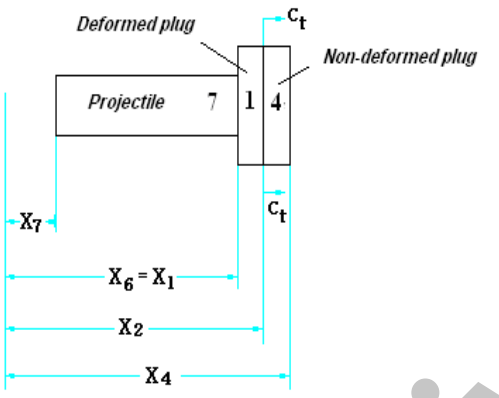

Fig. 3
Geometrical parameters in stage I.

Stage IIa: Projectile flattening - plug formation

This stage begins when the velocity of the projectile is less than the plastic wave speed and the plastic wave passes though the plug.

In this case the combination of the projectile, deformed and non-deformed plug constitute the controlled volume, Fig. 4. The linear momentum of the rigid and deformed part of the projectile and plug is:

$$\mathrm{M_7} = \rho_\mathrm{P} \cdot \mathrm{A_0} \cdot (\mathrm{X_6} - \mathrm{X_7}) \cdot \mathrm{V_7}` \quad (20)$$

$$\mathrm{M_4} = \rho_\mathrm{t} \cdot \mu \cdot \mathrm{A_0} \cdot (\mathrm{X_4} - \mathrm{X_2}) \cdot \mathrm{V_4} \quad (21)$$

$$M_\mathrm{I} = \rho_\mathrm{t} \cdot \mu \cdot \mathrm{A_0} \cdot (\mathrm{X_2} - \mathrm{X_1}) \cdot \mathrm{V_I} + \rho_\mathrm{p} \cdot \mathrm{C_p} \cdot (\mathrm{t\text{-}t_1}) \cdot \mathrm{V_I} \cdot \mathrm{A_0} \quad (22)$$

t_1 is the completion time of stage I.

Also:

$$\begin{cases} \mathrm{F} = \text{-}\pi \cdot \mathrm{D} \cdot (\mathrm{C_t} \cdot \mathrm{t}) \cdot \tau_\mathrm{f} \\ \varphi = 0 \end{cases} \quad (23)$$

By considering the momentum conservation principal (7), the following equations can be derived:

$$[\rho_t.\mu.A_0.C_t.t+\rho_p.A_0.C_P.(t-t_1)-M_C]\frac{dV_1}{dt}=-\pi.\mu^{1/2}.D_0.(C_t.t).\tau_f+\rho_P.A_0.C_P.(V_7-V_1)$$

$$\rho_t.\mu.A_0.C_t.(V_1-V_4)-[\frac{2}{3}.A_t-(K_t+B_t).Ln\frac{(X_4-T_0+C_t.t-X_1)}{C_t.t}].A_0.\mu+[A_P-B_P.Ln(\frac{H_P}{L_C})].A_0 \quad (24)$$

$$[\rho_t.(T_0-C_t.t).\mu.A_0]\frac{dV_4}{dt}=[\frac{2}{3}.A_t-(K_t+B_t).Ln\frac{(X_4-T_0+C_t.t-X_1)}{C_t.t}].A_0.\mu \quad (25)$$

where M_c is the mass of the separated projectile affected by shearing. And:

$$L_C=C_P.(t-t_1) \quad (26)$$

Due to the flattening of the projectile, the decrease in projectile's length is:

$$\frac{dL}{dt}=-C_p\cdot t \quad (27)$$

Based on Newton's second law we can write:

$$\frac{dV_7}{dt}=-\frac{A_P-B_P.Ln(\frac{H_P}{L_C})}{\rho_P.L} \quad (28)$$

The thickness of the flattened edge of the projectile is equal to:

$$H_p=X_1-X_6$$

This stage continues until $V_7-V_1\le 0$ or $V_1-V_4=0$.

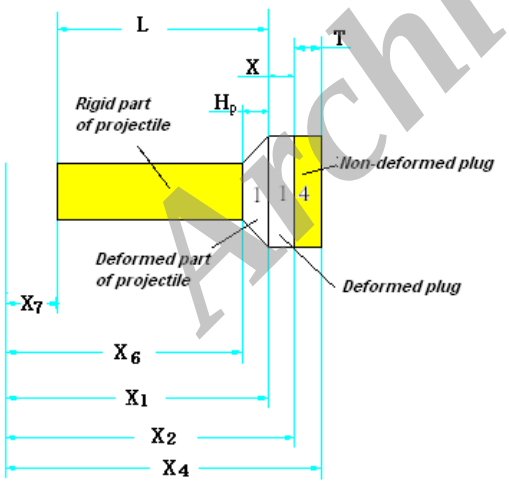

Fig. 4
Geometrical parameters in stage IIa.

Stage IIb: Projectile erosion - plug ejection

This stage begins when the relative velocity of the projectile is greater than the velocity of the plastic wave and the plastic wave reaches the end of plug.

In this stage, the momentum of the projectile and plug are:

$$M_7 = \rho_p \cdot A_0 \cdot (X_1\text{-}X_7) \cdot V_7$$
$$M_1 = \mu \cdot A_0 \cdot \rho_t \cdot T_0 \cdot V_1 \quad (29)$$

where as the net out flux of linear momentum through the control surface (erosion rate) is equal to:

$$\phi = \rho_p \cdot A_0 \cdot V_1 \cdot (V_7\text{-}V_1) \quad (30)$$

The external shear force exerted on the periphery of the deformed plug is equal to

$$F = -\pi\ D(x_4 - x_1)\tau_f \quad (31)$$

At this stage, the conservation of momentum principle leads to the following equations:

$$(\rho_t.\mu.A_0.T_0)\frac{dV_1}{dt} = -\pi.\mu^{1/2}.D_0.(X_3 + T_0 - X_1).\tau_f + \rho_P.A_0.(V_7 - V_1)^2 + (A_P + B_P).A_0 \quad (32)$$

$$\rho_t[\pi(\mu^{\frac{1}{2}}.\frac{D_0}{2} + C_S.t)^2 - \mu.A_0]\frac{dV_3}{dt} = \pi.\mu^{\frac{1}{2}}.\tau_{Yt}.D_0 - 2\pi.(\mu^{\frac{1}{2}}.\frac{D_0}{2} + C_S.t)(\tau_{Yt} + \rho_t.V_3.C_S) \quad (33)$$

$$\frac{dV_7}{dt} = -\frac{A_P + B_P}{\rho_P.L} \quad (34)$$

The rate of decrease in the length of the projectile is:

$$\frac{dL}{dt} = \frac{d}{dt}(X_1 - X_7) = V_1 - V_7 \quad (35)$$

The flattening of the projectile edge stops when propagation of the plastic stress wave in the projectile ceases.

Stage IIIa: Projectile rigid - plug formation

This stage begins when the plastic wave in the projectile vanishes while that in the plug is still propagating.

In this stage the linear momentum of the projectile, rigid and deformed plug are as follows:

$$M_4 = \rho_t \cdot \mu \cdot A_0 (X_4\text{-}X_2) \cdot V_4 \quad (36)$$
$$M_1 = \rho_p \cdot A_0 \cdot (X_6\text{-}X_7) \cdot V_7 + \rho_P \cdot C_P.(t_2 - t_1) \cdot A_0 \cdot V_1 + \rho_t \cdot \mu \cdot A_0 (X_2\text{-}X_1) \cdot V_1 \quad (37)$$

Also:

$$F = -\pi\ D(x_4 - x_1)\tau_f \quad (38)$$

$$\phi = 0 \quad (39)$$

In this stage, the linear momentum principal equations for projectile and plug can be simplified to:

$$[\rho_t.\mu.A_0.C_t.t + \rho_p.A_0.L_{12} + \rho_p.A_0.C_P.(t_2 - t_1) - M_C]\frac{dV_1}{dt} = -\pi.\mu^{1/2}.D_0.(C_t.t).\tau_f -$$
$$\rho_t.\mu.A_0.C_t.(V_1 - V_4) - [\frac{2}{3}.A_t - (K_t + B_t).Ln\frac{(X_4 - T_0 + C_t.t - X_1)}{C_t.t}]A_0.\mu) \quad (40)$$

$$[\rho_t.(T_0 - C_t.t).\mu.A_0]\frac{dV_4}{dt} = [(\frac{2}{3}.A_t - (K_t + B_t).Ln\frac{(X_4 - T_0 + C_t.t - X_1)}{C_t.t}].A_0.\mu \quad (41)$$

This stage continues until $V_1 - V_4 = 0$ or $V_7 - V_1 = 0$.

Stage IIIb: Projectile flattening - plug ejection

In this stage, a plastic wave may be propagated away from the interface into the projectile ($V_7 - V_1 < C_P$) while the plug is beginning to eject as a rigid body $V_r = V_1 - V_4 = 0$. Linear momentum principle equations as applied to rigid and deformed part of the projectile and plug are as below:

$$[\rho_t.\mu.A_0.T_0 + \rho_P.A_0(L_{C2} + C_P.(t - t_2) - M_C]\frac{dV_1}{dt} = -\pi.\mu^{1/2}.D_0.(X_3 + T_0 - X_1).\tau_f + \rho_P.A_0.C_P.(V_7 - V_1) + [A_P - B_P.Ln\frac{H_P}{L_{C2} + C_P.(t - t_2)}].A_0) \quad (42)$$

$$[\rho_t(\pi(\mu^{\frac{1}{2}}.\frac{D_0}{2} + C_S.t)^2 - \mu.A_0)]\frac{dV_3}{dt} = \pi.\mu^{\frac{1}{2}}.\tau_{Yt}.D_0 - 2\pi(\mu^{\frac{1}{2}}.\frac{D_0}{2} + C_S.t)(\tau_{Yt} + \rho_t.V_3.C_S) \quad (43)$$

$$\rho_P.L\frac{dV_7}{dt} = -(A_P - B_P.Ln\frac{H_P}{L_{C2} + C_P.(t - t_2)}) \quad (44)$$

L_{C2} is the length of projectile affected by plastic wave propagation at the end of second stage. Also:

$$\frac{dL}{dt} = -C_P.t \quad (45)$$

These stages continue up the time that following relation is maintained:

$V_7 - V_1 = 0$

Stage IV: Projectile rigid - plug ejection

When the interface pressure is not large enough to sustain a plastic wave in either the projectile or the target, it may be possible to continue plug ejection. In this stage, both the projectile and plug move as rigid bodies. The governing equations in this stage are:

$$\rho_t[\pi(\mu^{\frac{1}{2}}.\frac{D_0}{2} + C_S.t)^2 - \mu.A_0]\frac{dV_3}{dt} = \pi.\mu^{\frac{1}{2}}.\tau_{Yt}.D_0 - 2\pi.(\mu^{\frac{1}{2}}.\frac{D_0}{2} + C_S.t)(\tau_{Yt} + \rho_t.V_3.C_S) \quad (46)$$

$$[\rho_t.\mu.A_0.T_0 + \rho_P.A_0.(L_{12} + L_{C3}) - M_C]\frac{dV_1}{dt} = -\pi.\mu^{1/2}.D_0.(X_3 + T_0 - X_1).(\tau_f + \rho_t.V_3.C_S)` \quad (47)$$

L_{12} indicate rigid length of projectile and L_{C3} is the length of projectile affected by plastic stress wave propagation at the end of the third stage. This completion phase of the penetration process continues until $X_2 \geq X_3 + T_0$ or the plug is ejected from the target plate.

The perforation process is stopped when one of the following apply:

The velocity of the projectile reaches zero at one of the stages ($V_{p(t)} = 0$). Complete penetration does not occur.

The plug is ejected from the plate target i.e. $X_2 \geq X_3 + T_0$. Complete penetration occurs.

The projectile is eroded completely $L_{(t)} = 0$.

3 RESULTS AND DISCUSSION

The model developed above has been programmed in C++ language to solve the governing equations in these six stages. The program data input includes material constants, problem geometry and initial impact velocity of projectile. The computational output predicts residual velocity and length of projectile, ballistic limit velocity as well as plug mass and the diameter of the flattened projectile.

The validity of the model can be assessed with the experimental results other workers, for example with those from the experimental tests of Forrestal and Hanchak [14]. They performed several experiments to investigate the ballistic performance of HY-100 steel plates struck by flat-end 4340 steel cylindrical rod projectiles. The target thickness was 10.5 mm and the projectile diameter and length were 30mm and 282mm respectively. Based on the mechanical property of HY-100 and 4340 steel in reference [14], stress-strain constants have been computed and presented in Table 1.

Figs 5, 6 and 7, compare model predictions and experimental results for residual velocity, diameter of flattening area of projectile and mass of the plug at different initial velocities. It can be seen that there is good agreement between the two data sets. Geometrical parameters including projectile diameter and length and target thickness are shown in Table 2.

Also it is clear that, with increasing initial impact velocity, flatted diameter of the projectile will increase and consequently diameter and mass of plug will increase as well.

As expected, comparison of Figs. 5 and 6 shows that increasing the target thickness decreases the residual velocity of the projectile in all cases. Also from Figs. 5 and 7, decreasing the projectile mass decreases the residual velocity of projectile.

Previous theoretical models do not predict the diameter of the flattened area of projectile. This new model overcomes the problem, see Fig.6.

Table 1
Mechanical properties of projectile and target [16]

Material	ρ Kg/m^3	A Mpa	B Mpa
4340 St. (projectile)	7820	1170	318
HY-100 (target)	7800	739	418

Table 2
Geometrical parameters of projectile and target

	Target thickness (mm)	Projectile diameter (mm)	Projectile length (mm)	Projectile mass (gr)
Fig. 5	10.5	30.8	282	1560
Fig. 6	5.3	30.8	282	1560
Fig.7	10.5	30.8	89	520

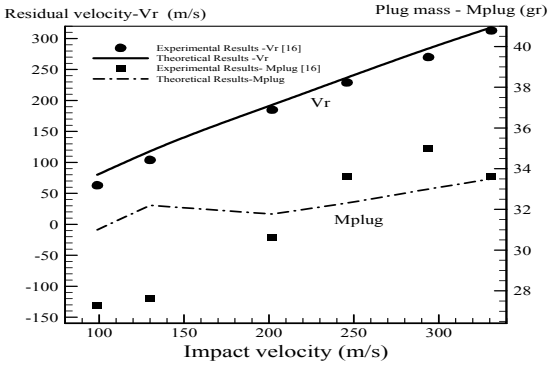

Fig. 5
Comparison of theoretical and experimental residual velocity and projectile flatted diameter at different initial velocities.

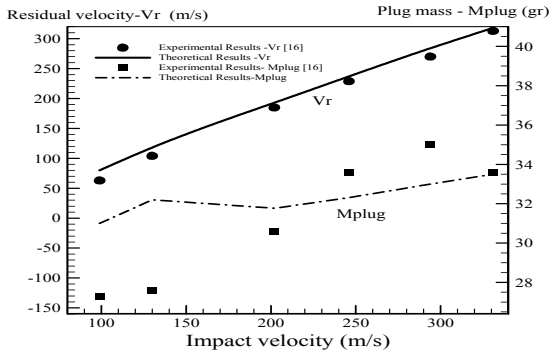

Fig. 6
Comparison of theoretical and experimental residual velocity and plug mass at different initial velocities.

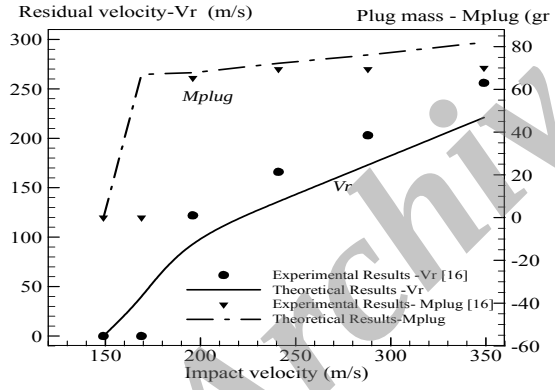

Fig. 7
Comparison of theoretical and experimental residual velocity and plug mass at different initial velocities.

The theoretical predictions of the model were also compared with the experimental results of Liu and Stronge [15]. Their target was made of 3.03mm thick Al 1200. The density was 2700 Kg/m^3 and Stress-strain constant data are assumed as $A_t = 115\ Mpa$, $B_p = 200\ Mpa$. The projectiles material was deformable and made from three different materials 1200 AL, 6063 TF and 6061 T6 Aluminum alloy with the mass of 3.8 gr, diameter of 12.5 mm and length of 11.46 mm. Table 3 lists stress- strain constants for the projectile. Table 4 lists the experimental and predicted values of ballistic limit velocity (V_b) and residual length (X) of the projectile. It can be seen that there is close agreement between the data sets and thus provides confidence in the validity of the model. Model predictions can also be compared with the experimental data obtained by Liu and Stronge [15] for a flat-ended projectile made of hardened steel. The hardened steel projectile experienced negligible inelastic deformation during the impact process and consequently can be considered as a rigid projectile. The coefficients of stress-strain constants for hardened steel are $A_p = 1540\ Mpa$, $B_p = 474\ Mpa$. These coefficients have also been used by Borvik et al [16] for Arne tool steel.

Table 5 lists the values of ballistic limit velocity for different target materials and thicknesses and of target and different lengths of projectile along with model results. It is clear that for hardened steel projectiles the theoretical ballistic limit velocity shows good agreement with experimental results. Tables 4 and 5 show that the ratio of the plate thickness to the projectile diameter is less than one, i.e. the target is thin. For thin metallic targets especially at the near of ballistic limit velocity, the deformation on the outside of the shear plug is high. In the new theoretical model, deformation of outside of the shear plug is considered.

The present model is only valid for the perforation controlled by the shear plugging failure mode with or without the presence of deformation outside the shear plug. For the experiment test of Liu and Stronge [15], if the plate thickness is smaller than or as large as the projectile diameter, the rupture mechanism is plugging.

It appears valid to use rigid-plastic linear work hardening model for the projectile and target material. However, it should be noted that the local material response during a penetration/perforation process may involve large plastic deformation, strain rate hardening and temperature or damage softening. The current model does not include these complex factors.

Table 3
Stress- strain constant data of projectile [17]

Material type	$A(Mpa)$	$B(Mpa)$
1200 Al	60	376
6063 TF	150	465
6061 T6	320	956

Table 4
Comparison of ballistic limit velocity and residual length of projectile between theoretical and experimental results [17]

Projectile material	Experimental results [17]		New theoretical model	
	$X(mm)$	$V_b(m/s)$	$X(mm)$	$V_b(m/s)$
1200 AL	5.7	354 ± 7	4.9	342
6063 TF	5.7	319 ± 7	6.7	323
6061 T6	7.8	247 ± 3	6.68	263

Table 5
Comparison of theoretical and experimental [17] ballistic limit velocity

Projectile $m_p(gr)$	Projectile $D_0(mm)$	Target Thickness(mm)	Target material	$A_t(Mpa)$	$B_t(Mpa)$	Experimental Ballistic limit velocity [17] $V_b(m/s)$	Theoretical Ballistic limit velocity $V_b(m/s)$
23.6	12.5	6.27	2014Al	288	350	147 ± 3	140
24.6	12.5	3.25	2014Al	302	900	122 ± 5	115
9.7	12.5	3.03	1200Al	115	200	145 ± 3.5	140
9.7	12.5	6.42	1200Al	114	275	218 ± 5	212
3.8	12.5	3.03	1200Al	115	200	229.5 ± 5.5	214
3.8	12.5	6.42	1200Al	114	275	357.5 ± 5.5	360

4 CONCLUSIONS

The theoretical model presented in this paper is a new method which analyzes perforation of a thin metallic target struck by a blunt projectile by considering plastic wave propagation. Comparison with experimental results shows that the proposed theoretical model can successfully predict the values of residual velocity, ballistic limit velocity, residual length and diameter of flatted area of the projectile and plug mass.

REFERENCES

[1] Backman M. E., Goldsmith W., 1978, The mechanics of penetration of projectiles into targets, *International Journal of Engineering Science* 16:1-99.

[2] Anderson J. R., Morris B. L., Littlefield D. L., 1992, A penetration mechanics database, *Southwest Research Institute Report* 3593/001.

[3] Goldsmith W., 1999, Non ideal projectile impact on targets, *International Journal of Impact Engineering* **22**: 95-395.

[4] Whiffin A.C., 1948, The use of flat-ended projectiles for determining dynamical yield stress. II. Test on various metallic materials, *Proceedings the Royal Society* **194** (1038): 300-322.

[5] Taylor G.I., 1948, The use of flat-ended projectiles for determining dynamical yield stress. I. Theoretical consideration, *Proceedings the Royal Society* **194** (1038): 289-299.

[6] Hashmi M. S. J., Thompson P.J., 1977, A numerical method of analysis for the mushrooming of flat- ended projectiles impinging on a flat rigid anvil, *International Journal of Mechanical Sciences* **19**: 273-283.

[7] Awerbuch J., Bodner S.R., 1974, Analysis of the mechanics of perforation of projectiles in metallic plates, *International Journal of Solids and Structures* **10**(1): 671-684.

[8] Ravid M., Bodner S. R., 1983, Dynamic perforation of viscoplastic plates by rigid projectiles, *International Journal of Engineering Science* **21**: 577-591.

[9] Liss J., Goldsmith W., Kelly J.M., 1983, A phenomenological penetration model of plates, *International Journal of Impact Engineering* **1**(4): 321-341.

[10] Wenxue Y., Lanting Z., Xiaoqing M. , Strong W. J., 1983, Plate perforation by deformable projectiles- a plastic wave theory, *International Journal of Impact Engineering* **1**(4): 393-412.

[11] Chen X.W., Li Q.M., 2003, Shear plugging and perforation of ductile circular plates struck by a blunt projectile, *International Journal of Impact Engineering* **28**: 513-536.

[12] Zukas J.A., 1990, High Velocity Impact Dynamic, John Wily and Sons.

[13] Lai W.M., Rubin D., Kremp E., 1999, *Introduction to Continuum Mechanics*, Third Edition, Butterworth-Heinemann.

[14] Forrestal M.J. , Hanchak S., 1999, Penetration experiments on HY-100 steel plates with 4340 Rc 38 and maraging T-250 steel rod projectiles, *International Journal of Impact Engineering* **22**: 923-933.

[15] Liu D., Stronge W.J., 2000, Ballistic limit of metal plates struck by blunt deformable missiles: experiments, *International Journal of Solids and Structures* **37**: 1403-1423.

[16] Borvik T., Langseth M., Hopperstad O.S., 1999, Ballistic penetration of steel plates, *International Journal of Impact Engineering* **22**:855-886.